Sanford Underground Research Facility: *Location of DUNE*

Modified TM2 for Reproducing All Best-Fit Values of Neutrino Mixing Angles

Michael Fodroci

with T. Kitabayashi

NPN2026 Mito, Japan

TOKAI UNIVERSITY

This Work: PTEP 2026 (arXiv:2511.15111)

Outline

- Motivation
- Modification to TBM
- Predictions of Modified TM2
  - Benchmark Points
  - Predicted Mixing Angles vs NuFit
  - Effective $0\nu\beta\beta$ Majorana Mass
- Magic Texture Symmetry of Modified TM2
- Conclusions

From my time as a DUNE member, underground at Sanford Lab
Left to right: Myself, Dr. Juergen Reichenbacher, Tyler Rath

Motivation

- **Next generation experiments** (i.e. DUNE, JUNO, T2HK) leading to **precision measurements** of neutrino oscillation parameters
- Searching for models capable of accommodating both **nonzero reactor angle** and **solar angle below ⅓**
- Desire a model that is also robust against some changes in central values

		Normal Ordering (best fit)		Inverted Ordering ($\Delta\chi^2 = 5.9$)	
		bfp $\pm 1\sigma$	3σ range	bfp $\pm 1\sigma$	3σ range
IC24 with SK atmospheric data	$\sin^2\theta_{12}$	$0.3088^{+0.0067}_{-0.0066}$	$0.2893 \to 0.3295$	$0.3088^{+0.0067}_{-0.0066}$	$0.2893 \to 0.3295$
	$\theta_{12}/^\circ$	$33.76^{+0.42}_{-0.41}$	$32.54 \to 35.03$	$33.76^{+0.42}_{-0.41}$	$32.54 \to 35.03$
	$\sin^2\theta_{23}$	$0.470^{+0.017}_{-0.014}$	$0.435 \to 0.584$	$0.550^{+0.013}_{-0.016}$	$0.439 \to 0.584$
	$\theta_{23}/^\circ$	$43.29^{+0.96}_{-0.79}$	$41.27 \to 49.86$	$47.90^{+0.73}_{-0.92}$	$41.51 \to 49.83$
	$\sin^2\theta_{13}$	$0.02248^{+0.00055}_{-0.00059}$	$0.02064 \to 0.02418$	$0.02262^{+0.00057}_{-0.00056}$	$0.02093 \to 0.02441$
	$\theta_{13}/^\circ$	$8.62^{+0.11}_{-0.11}$	$8.26 \to 8.95$	$8.65^{+0.11}_{-0.11}$	$8.32 \to 8.99$
	$\delta_{CP}/^\circ$	212^{+26}_{-36}	$125 \to 365$	274^{+22}_{-25}	$203 \to 335$
	$\frac{\Delta m^2_{21}}{10^{-5}\ \mathrm{eV}^2}$	$7.537^{+0.094}_{-0.10}$	$7.236 \to 7.823$	$7.537^{+0.094}_{-0.10}$	$7.236 \to 7.822$
	$\frac{\Delta m^2_{3\ell}}{10^{-3}\ \mathrm{eV}^2}$	$+2.511^{+0.021}_{-0.020}$	$+2.450 \to +2.576$	$-2.483^{+0.020}_{-0.020}$	$-2.547 \to -2.421$

NuFit 2025: http://www.nu-fit.org/

$$\sin^2\theta_{12,\,JUNO} = 0.3092 \pm 0.0087$$

JUNO Collaboration et al. First measurement of reactor neutrino oscillations at JUNO, 2025

Modification to TBM

$$U_{\rm TBM} = \begin{pmatrix} \sqrt{\frac{2}{3}} & \sqrt{\frac{1}{3}} & 0 \\ -\sqrt{\frac{1}{6}} & \sqrt{\frac{1}{3}} & -\sqrt{\frac{1}{2}} \\ -\sqrt{\frac{1}{6}} & \sqrt{\frac{1}{3}} & \sqrt{\frac{1}{2}} \end{pmatrix}$$

$$U^0_{\rm MTBM} = \begin{pmatrix} \sqrt{\frac{2}{3}} & \sqrt{\frac{1}{3}+\epsilon} & 0 \\ -\sqrt{\frac{1}{6}} & \sqrt{\frac{1}{3}} & -\sqrt{\frac{1}{2}} \\ -\sqrt{\frac{1}{6}} & \sqrt{\frac{1}{3}} & \sqrt{\frac{1}{2}} \end{pmatrix}$$

$$U_{\rm MTBM} = \begin{pmatrix} \sqrt{\frac{2}{3}+x_1} & \sqrt{\frac{1}{3}+\epsilon} & 0 \\ -\sqrt{\frac{1}{6}+x_2} & \sqrt{\frac{1}{3}+x_3} & -\sqrt{\frac{1}{2}+x_4} \\ -\sqrt{\frac{1}{6}+x_5} & \sqrt{\frac{1}{3}+x_6} & \sqrt{\frac{1}{2}+x_7} \end{pmatrix},$$

$$U_{\rm MTBM} = \begin{pmatrix} \sqrt{\frac{2}{3}-\epsilon} & \sqrt{\frac{1}{3}+\epsilon} & 0 \\ -\sqrt{\frac{1}{6}+\frac{\epsilon}{2}} & \sqrt{\frac{1}{3}-\frac{\epsilon}{2}} & -\sqrt{\frac{1}{2}} \\ -\sqrt{\frac{1}{6}+\frac{\epsilon}{2}} & \sqrt{\frac{1}{3}-\frac{\epsilon}{2}} & \sqrt{\frac{1}{2}} \end{pmatrix}$$

$$x_4 = 0, \quad x_7 = 0$$

Modification to TBM

$$\tilde{U}_{\mathrm{TM}_2} = \begin{pmatrix} \sqrt{\frac{2}{3}} - \epsilon \cos\theta & \sqrt{\frac{1}{3}+\epsilon} & \sqrt{\frac{2}{3}} - \epsilon \sin\theta \\ -\sqrt{\frac{1}{6}+\frac{\epsilon}{2}}\cos\theta + \frac{e^{-i\phi}\sin\theta}{\sqrt{2}} & \sqrt{\frac{1}{3}-\frac{\epsilon}{2}} & -\sqrt{\frac{1}{6}+\frac{\epsilon}{2}}\sin\theta - \frac{e^{-i\phi}\cos\theta}{\sqrt{2}} \\ -\sqrt{\frac{1}{6}+\frac{\epsilon}{2}}\cos\theta - \frac{e^{-i\phi}\sin\theta}{\sqrt{2}} & \sqrt{\frac{1}{3}-\frac{\epsilon}{2}} & -\sqrt{\frac{1}{6}+\frac{\epsilon}{2}}\sin\theta + \frac{e^{-i\phi}\cos\theta}{\sqrt{2}} \end{pmatrix}$$

$$s^2_{12} = \frac{1+3\epsilon}{3-(2-3\epsilon)\sin^2\theta},$$

$$s^2_{23} = \frac{1}{2}\left(1 + \frac{\sqrt{3(1+3\epsilon)}\sin 2\theta\cos\phi}{3-(2-3\epsilon)\sin^2\theta}\right),$$

$$s^2_{13} = \left(\frac{2}{3}-\epsilon\right)\sin^2\theta,$$

$$\tan\delta = \frac{4+3\epsilon+(2-3\epsilon)\cos 2\theta}{2-3\epsilon+(4+3\epsilon)\cos 2\theta}\tan\phi.$$

Benchmark Points

NO:

$$(\theta, \phi, \epsilon) = (167.76^\circ, 287.62^\circ, -0.03216)$$

$$(s^2_{12}, s^2_{23}, s^2_{13}, \delta) = (0.308, 0.470, 0.02215, 287.6^\circ)$$

IO:

$$(\theta, \phi, \epsilon) = (169.71^\circ, 239.50^\circ, -0.0322)$$

$$(s^2_{12}, s^2_{23}, s^2_{13}, \delta) = (0.308, 0.550, 0.02231, 239.5^\circ)$$

Modification to TBM

$$\tilde{U}_{\mathrm{TM}_2} = \begin{pmatrix} \sqrt{\frac{2}{3}} - \epsilon\cos\theta & \sqrt{\frac{1}{3}+\epsilon} & \sqrt{\frac{2}{3}} - \epsilon\sin\theta \\ -\sqrt{\frac{1}{6}+\frac{\epsilon}{2}}\cos\theta + \frac{e^{-i\phi}\sin\theta}{\sqrt{2}} & \sqrt{\frac{1}{3}-\frac{\epsilon}{2}} & -\sqrt{\frac{1}{6}+\frac{\epsilon}{2}}\sin\theta - \frac{e^{-i\phi}\cos\theta}{\sqrt{2}} \\ -\sqrt{\frac{1}{6}+\frac{\epsilon}{2}}\cos\theta - \frac{e^{-i\phi}\sin\theta}{\sqrt{2}} & \sqrt{\frac{1}{3}-\frac{\epsilon}{2}} & -\sqrt{\frac{1}{6}+\frac{\epsilon}{2}}\sin\theta + \frac{e^{-i\phi}\cos\theta}{\sqrt{2}} \end{pmatrix}$$

NuFit 2025: http://www.nu-fit.org/

IC24 with SK atmospheric data		Normal Ordering (best fit)		Inverted Ordering ($\Delta\chi^2 = 5.9$)	
		bfp $\pm 1\sigma$	3σ range	bfp $\pm 1\sigma$	3σ range
	$\sin^2\theta_{12}$	$0.3088^{+0.0067}_{-0.0066}$	$0.2893 \to 0.3295$	$0.3088^{+0.0067}_{-0.0066}$	$0.2893 \to 0.3295$
	$\theta_{12}/^\circ$	$33.76^{+0.42}_{-0.41}$	$32.54 \to 35.03$	$33.76^{+0.42}_{-0.41}$	$32.54 \to 35.03$
	$\sin^2\theta_{23}$	$0.470^{+0.017}_{-0.014}$	$0.435 \to 0.584$	$0.550^{+0.013}_{-0.016}$	$0.439 \to 0.584$
	$\theta_{23}/^\circ$	$43.29^{+0.96}_{-0.79}$	$41.27 \to 49.86$	$47.90^{+0.73}_{-0.92}$	$41.51 \to 49.83$
	$\sin^2\theta_{13}$	$0.02248^{+0.00055}_{-0.00059}$	$0.02064 \to 0.02418$	$0.02262^{+0.00057}_{-0.00056}$	$0.02093 \to 0.02441$
	$\theta_{13}/^\circ$	$8.62^{+0.11}_{-0.11}$	$8.26 \to 8.95$	$8.65^{+0.11}_{-0.11}$	$8.32 \to 8.99$
	$\delta_{\mathrm{CP}}/^\circ$	212^{+26}_{-36}	$125 \to 365$	274^{+22}_{-25}	$203 \to 335$
	$\frac{\Delta m^2_{21}}{10^{-5}\ \mathrm{eV}^2}$	$7.537^{+0.094}_{-0.10}$	$7.236 \to 7.823$	$7.537^{+0.094}_{-0.10}$	$7.236 \to 7.822$
	$\frac{\Delta m^2_{3\ell}}{10^{-3}\ \mathrm{eV}^2}$	$+2.511^{+0.021}_{-0.020}$	$+2.450 \to +2.576$	$-2.483^{+0.020}_{-0.020}$	$-2.547 \to -2.421$

Benchmark Points

NO:

$$(\theta, \phi, \epsilon) = (167.76^\circ, 287.62^\circ, -0.03216)$$

$$(s^2_{12}, s^2_{23}, s^2_{13}, \delta) = (0.308, 0.470, 0.02215, 287.6^\circ)$$

IO:

$$(\theta, \phi, \epsilon) = (169.71^\circ, 239.50^\circ, -0.0322)$$

$$(s^2_{12}, s^2_{23}, s^2_{13}, \delta) = (0.308, 0.550, 0.02231, 239.5^\circ)$$

Predictions of Modified TM2: Predicted Mixing Angles vs NuFit

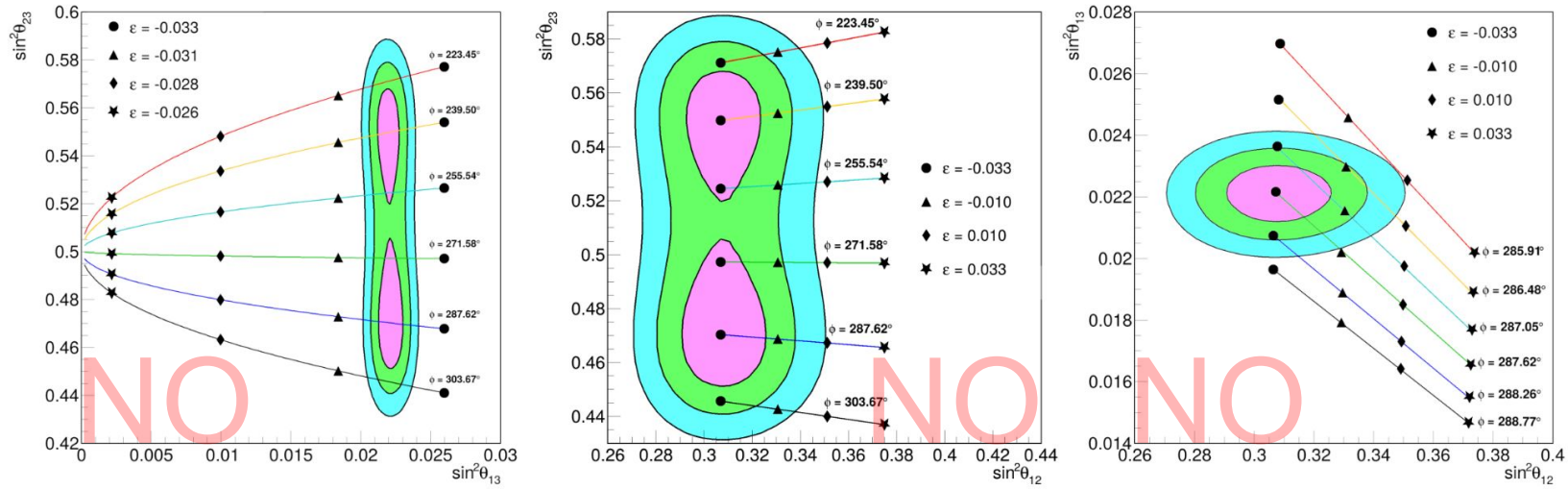

Figure 1: NO case predictions of the modified TM_2 model for fixed $\sin^2\theta_{12}$(left), fixed $\sin^2\theta_{13}$(middle), and fixed $\sin^2\theta_{23}$(right). Shaded regions correspond to NuFIT [111] 1σ(magenta), 2σ(green), and 3σ(cyan) allowed regions. Points of the same shape indicated equivalent values of ϵ while the various colored curves indicate level lines of ϕ. Points are restricted to $-\frac{1}{30} \leq \epsilon \leq \frac{1}{30}$ and $\frac{3}{4}\pi \leq \theta \leq \pi$.

Using Data From : NuFit 2025 http://www.nu-fit.org/

Predictions of Modified TM2: Predicted Mixing Angles vs NuFit

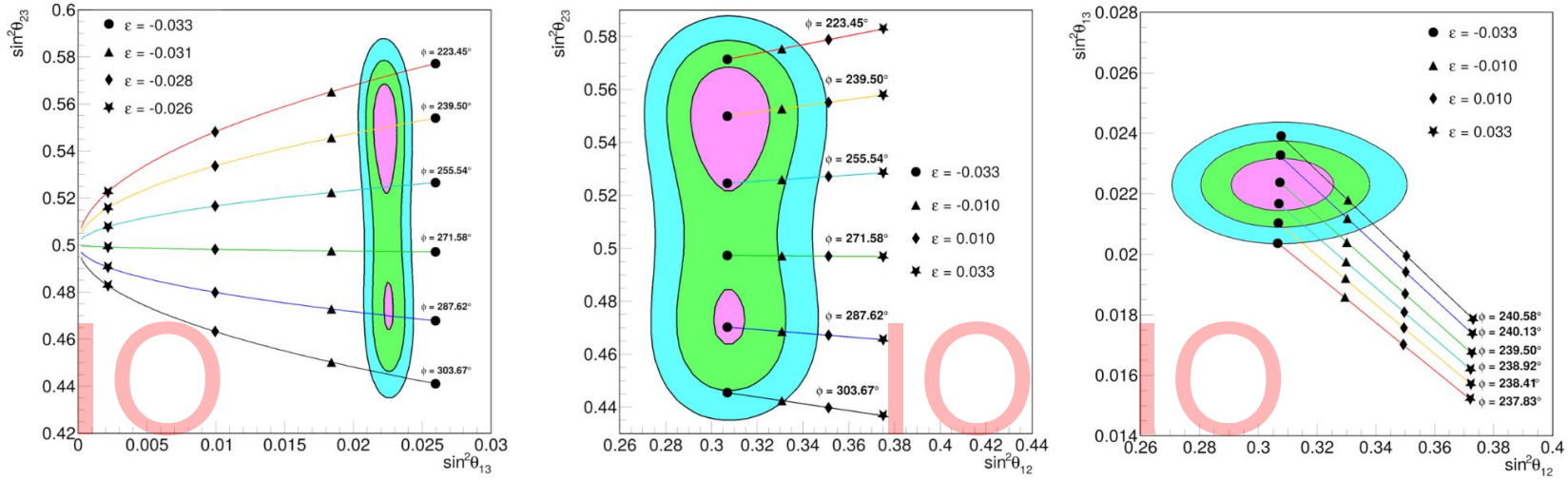

Figure 2: IO case predictions of the modified TM_2 model for fixed $\sin^2\theta_{12}$(left), fixed $\sin^2\theta_{13}$(middle), and fixed $\sin^2\theta_{23}$(right). Shaded regions correspond to NuFIT [111] 1σ(magenta), 2σ(green), and 3σ(cyan) allowed regions. Points of the same shape indicated equivalent values of ϵ while the various colored curves indicate level lines of ϕ. Points are restricted to $-\frac{1}{30} \leq \epsilon \leq \frac{1}{30}$ and $\frac{3}{4}\pi \leq \theta \leq \pi$.

Using Data From : NuFit 2025 http://www.nu-fit.org/

Predictions of Modified TM2:Majorana CP Phases

- Plot shows **ranges of upper limits on effective $m_{\beta\beta}$** probeable by various **current / next generation $0\nu\beta\beta$** experiments
- Plotted as function of Majorana phase alpha with the lightest neutrino mass set to zero
- Like other such models, expected that **full IO region soon probeable**, but **NO not yet accessible**

NO:
$$\cos 2\alpha = \frac{9m_{\beta\beta}^2 - (1+3\epsilon)^2 m_2^2 - (2-3\epsilon)^2 m_3^2 \sin^4\theta}{2(2+3\epsilon-9\epsilon^2) m_2 m_3 \sin^2\theta}$$

IO:
$$\cos 2\alpha = \frac{9m_{\beta\beta}^2 - (1+3\epsilon)^2 m_2^2 - (2-3\epsilon)^2 m_1^2 \cos^4\theta}{2(2+3\epsilon-9\epsilon^2) m_1 m_2 \cos^2\theta}$$

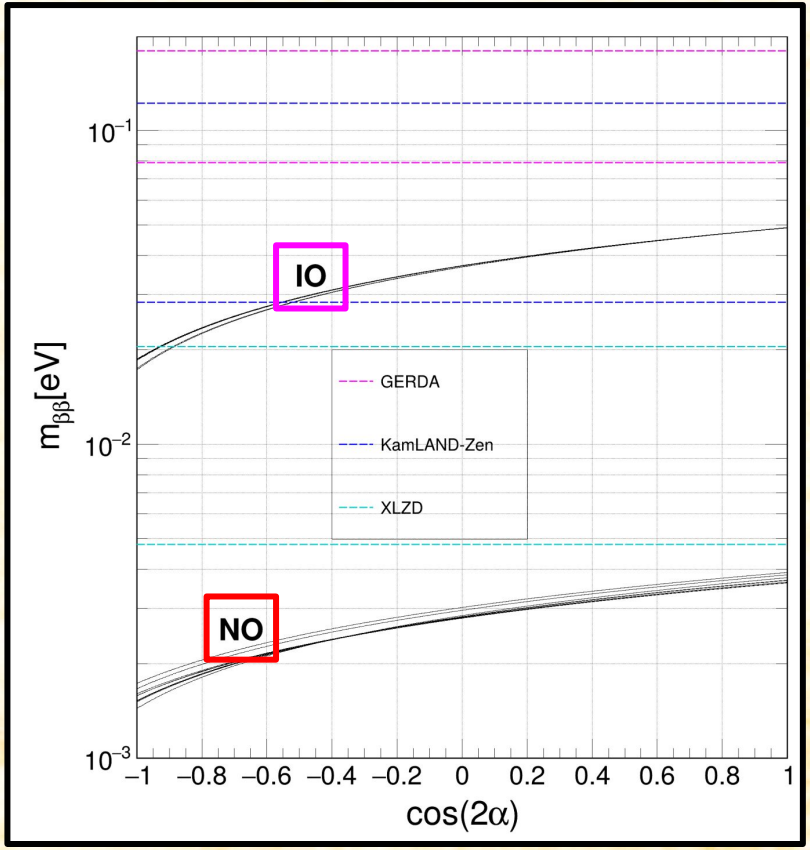

Magic Texture Symmetry of Light Neutrino Mass Matrix Under Modified TM2

- Typical TM2 li**ght neutrino mass matrix** after applying see-saw mechanism has "**Magic Texture Symmetry"**
- Our modification **breaks this symmetry**
- We explore the degree of this breaking as a function of the Majorana phase alpha

$$M_{\text{magic}} = \begin{pmatrix} a & b & c \\ b & d & a+c-d \\ c & a+c-d & b-c+d \end{pmatrix}$$

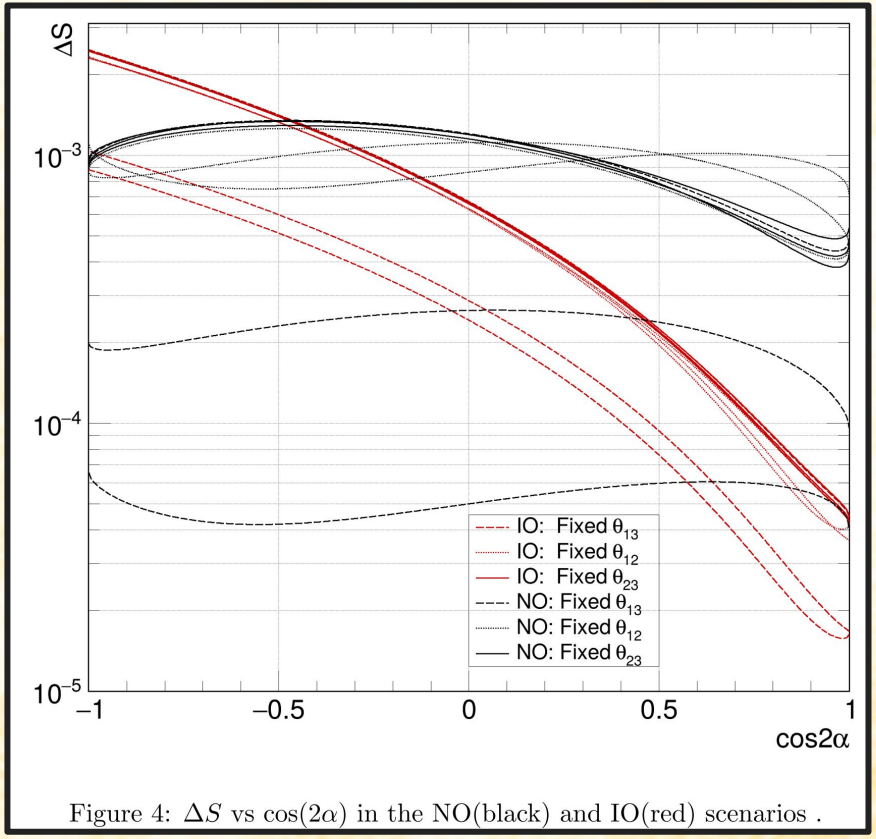

Figure 4: ΔS vs $\cos(2\alpha)$ in the NO(black) and IO(red) scenarios .

Conclusions

- Our model represents **viable phenomenological approach** to accurately reproducing all the current best fit values of the mixing angles - and is furthermore **robust against small changes to these central values**
- The predictions for the possible range of $m_{\beta\beta}$ are in agreement with other similar models
- We have also explored some other properties of this model such as its deviation from magic texture symmetry

- Please keep an eye open for my upcoming publication on the capabilities of **DUNE** to measure the **solar ν_e day/night asymmetry** and probe the **density/chemical structure of Earth** as well as **supernova burst neutrino matter effects**

This Work: " Modified TM2 for Reproducing All Best-Fit Values of Neutrino Mixing Angles"

This Work: PTEP 2026 (arXiv:2511.15111)

TOKAI UNIVERSITY

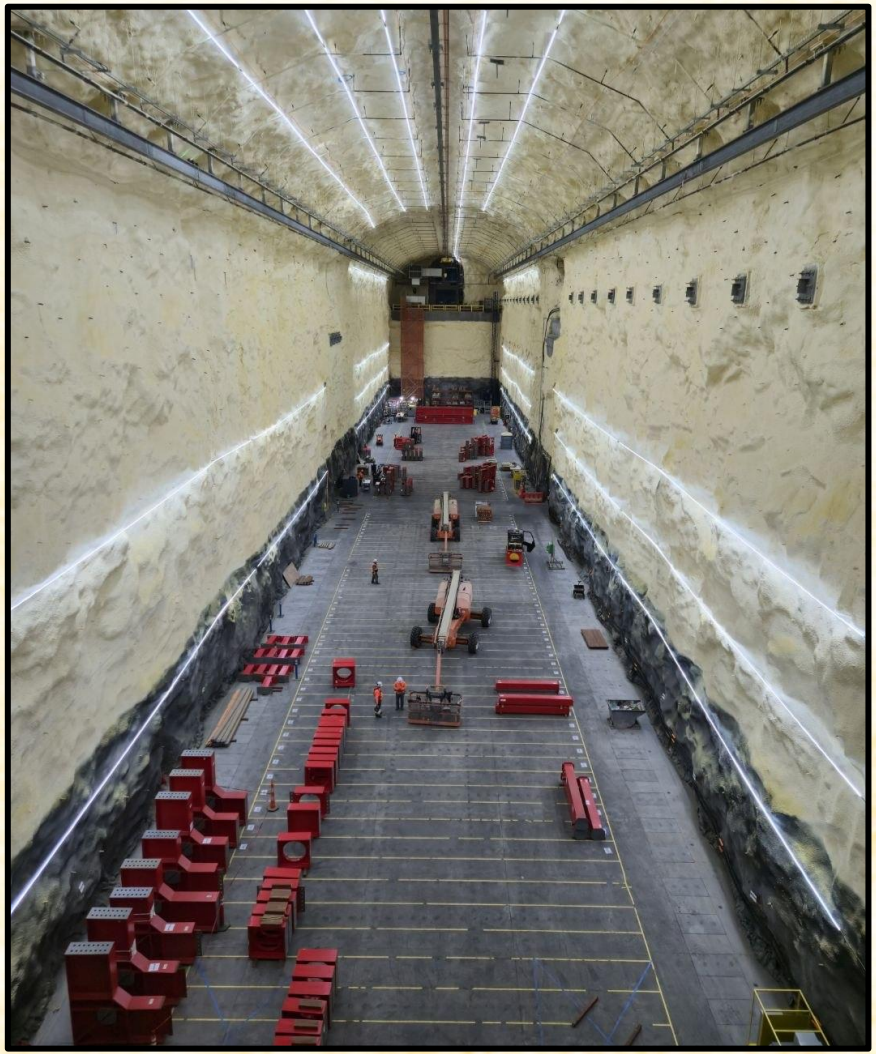

Courtesy of
Dr. Jairo Rodriguez Rondon

Appendix: A

3.3.2 Predictions of Modified TM_2 Model Around NuFIT 3σ Allowed Regions

While it is clear that the parameters of the modified TM_2 mixing model may be tuned to match best-fit data, one may wonder how exactly it manages to reproduce the observed mixing angles. It is also interesting to see for what region of parameter space the values predicted by the modified TM_2 model remain close to the current best-fit values. In order to investigate this we present six different plots in Figures 1 and 2 wherein we have held fixed one of the three mixing angles while varying $\theta/\epsilon/\phi$ in both the NO and IO cases. The predictions of our model under various ranges of parameters are then overlaid with the $1/2/3\sigma$ regions given by NuFit [111]

In the left hand figures we set $\sin^2\theta_{12}$ equal to its best-fit value as per Eqs.(7) and (8) as well as set ϕ to the values in Eqs.(27) and (29). We then vary ϵ between $-\frac{1}{30}$ and $\frac{1}{30}$ and use Eq.(23) to compute θ - only keeping solutions that fall in the range $\frac{3}{4}\pi \leq \theta \leq \pi$. This is then repeated for several reasonable values of ϕ around the intial value. For the middle figures, $\sin^2\theta_{13}$ is fixed at the best-fit value instead and the process repeated.

For the right most figures corresponding to a fixed $\sin^2\theta_{23}$ the situation is not as simple. Inspection of Eq.(24) shows this same process cannot be repeated as easily due to the more complicated form of this equation. Therefore, in order to proceed with the analysis we take Eq.(24) and rewrite it as follows.

$$s^2_{23} = \frac{1}{2}\left(1 + \frac{\sqrt{3}\sqrt{1+3\epsilon}\sin 2\theta\cos\phi}{3-(2-3\epsilon)\sin^2\theta}\right) \tag{31}$$

Using the fact that 3ϵ is a small parameter we replace the root containing ϵ with its Taylor series expansion.

$$s^2_{23} = \frac{1}{2}\left(1 + \frac{\sqrt{3}(1+\frac{3\epsilon}{2}-\frac{9\epsilon^2}{8}+\ \ldots\ )\sin 2\theta\cos\phi}{3-(2-3\epsilon)\sin^2\theta}\right) \tag{32}$$

Truncating at the third order term leaves us with a much more manageable expression which is quadratic in ϵ.

$$s^2_{23} = \frac{1}{2}\left(1 + \frac{\sqrt{3}(1+\frac{3\epsilon}{2}-\frac{9\epsilon^2}{8})\sin 2\theta\cos\phi}{3-(2-3\epsilon)\sin^2\theta}\right) \tag{33}$$

On the relevant range of ϵ the error at the third order can be shown to be less than 1%. Next, using this new experssion, we again set ϕ to the values from Eqs.(27)/(29) and then vary θ between $\frac{3}{4}\pi$ and π. We solve the quadratic at each value of θ and keep only the solutions for which ϵ falls between $-\frac{1}{30}$ and $\frac{1}{30}$. This is the reverse of the left and middle plots where we plugged in a value for ϵ to compute θ. This is again repeated for several reasonable values of ϕ around the initial value.

Appendix: B

With respect to the modified TM_2 mixing in Eq.(22), the Majorana CP phases and the effective Majorana neutrino mass for neutrinoless double beta decay are related through

$$\begin{aligned} m_{\beta\beta} &= \sum_i (\tilde{U}_{\mathrm{TM}_2})^2_{ei} m_i \\ &= \frac{1}{9}\left\{(2-3\epsilon)^2 m_1^2 \cos^4\theta + (1+3\epsilon)^2 m_2^2 + (2-3\epsilon)^2 m_3^2 \sin^4\theta \right. \\ &\quad +2(2+3\epsilon-9\epsilon^2) m_1 m_2 \cos^2\theta \cos 2\alpha + 2(2+3\epsilon-9\epsilon^2) m_2 m_3 \sin^2\theta \cos 2(\alpha-\beta) \\ &\quad \left. +2(2-3\epsilon)^2 m_1 m_3 \cos^2\theta \sin^2\theta \cos 2\beta \right\}. \end{aligned} \tag{34}$$

Because each of the ei elements are independent of ϕ in $\tilde{U}_{\mathrm{TM}_2}$, $m_{\beta\beta}$ is also independent of ϕ.

If one of the neutrino masses vanishes, such as in the minimal seesaw model, only one physical Majorana CP phase survives. More concretely, we can take the diagonal neutrino mass matrix to be $M_{\mathrm{diag}} = \mathrm{diag.}(0, m_2 e^{2i\alpha}, m_3)$ for the NO case and $M_{\mathrm{diag}} = \mathrm{diag.}(m_1, m_2 e^{2i\alpha}, 0)$ for IO. This way, the Majorana CP phase is estimated as

$$\cos 2\alpha = \frac{9m_{\beta\beta}^2 - (1+3\epsilon)^2 m_2^2 - (2-3\epsilon)^2 m_3^2 \sin^4\theta}{2(2+3\epsilon-9\epsilon^2) m_2 m_3 \sin^2\theta} \tag{35}$$

for $m_1 = 0$ and

$$\cos 2\alpha = \frac{9m_{\beta\beta}^2 - (1+3\epsilon)^2 m_2^2 - (2-3\epsilon)^2 m_1^2 \cos^4\theta}{2(2+3\epsilon-9\epsilon^2) m_1 m_2 \cos^2\theta} \tag{36}$$

for $m_3 = 0$.

In Figure 3 we plot $m_{\beta\beta}$ versus $\cos 2\alpha$ in the NO/IO case using the appropriate rearrangement of Eq.(35)/Eq.(36). We have done this at 3 points for each of the graphs in Figures and - one point at the best-fit value as well as a point sampling the 2σ and 3σ allowed regions, all three of which are taken at distinct ϕ values. While, as noted, $m_{\beta\beta}$ is independent of ϕ, this is not the case for the magic texture symmetry breaking parameter, ΔS, which will be investigated using the same set of values in 3.3.4. In the NO case this corresponds to the following range of model parameters:

Appendix: C

$$\text{NO Fixed } \theta_{13}: \begin{cases} 169.56^\circ \leq \theta \leq 169.75^\circ \\ 223.45^\circ \leq \phi \leq 287.62^\circ \\ -0.0333 \leq \epsilon \leq -0.0079 \end{cases},$$

$$\text{NO Fixed } \theta_{12}: \begin{cases} 169.76^\circ \leq \theta \leq 170.12^\circ \\ 223.45^\circ \leq \phi \leq 287.62^\circ \\ -0.0321 \leq \epsilon \leq -0.0317 \end{cases},$$

$$\text{NO Fixed } \theta_{23}: \begin{cases} 169.56^\circ \leq \theta \leq 169.75^\circ \\ 223.45^\circ \leq \phi \leq 287.62^\circ \\ -0.0325 \leq \epsilon \leq -0.0331 \end{cases}.$$

While in the IO case this corresponds to:

$$\text{IO Fixed } \theta_{13}: \begin{cases} 169.61^\circ \leq \theta \leq 169.72^\circ \\ 239.50^\circ \leq \phi \leq 303.67^\circ \\ -0.0332 \leq \epsilon \leq -0.0199 \end{cases},$$

$$\text{IO Fixed } \theta_{12}: \begin{cases} 169.71^\circ \leq \theta \leq 169.72^\circ \\ 239.50^\circ \leq \phi \leq 303.67^\circ \\ -0.0322 \leq \epsilon \leq -0.0321 \end{cases},$$

$$\text{IO Fixed } \theta_{23}: \begin{cases} 169.50^\circ \leq \theta \leq 170.17^\circ \\ 237.83^\circ \leq \phi \leq 240.13^\circ \\ -0.0331 \leq \epsilon \leq -0.0330 \end{cases}.$$

Appendix: D

Furthermore, in Figure 3, we have included several notable ranges of the upper limit on $m_{\beta\beta}$ from current and future experiments. In magenta we show the range taken from the final results of GERDA [112] at 90% C.L.

$$m_{\beta\beta,\,\mathrm{GERDA}} < 79\,[\mathrm{meV}] - 180\,[\mathrm{meV}]. \tag{37}$$

In dark blue we show the predicted 90% C.L. range for the planned XLZD [113] experiment

$$m_{\beta\beta,\,\mathrm{XLZD}} < 4.8\,[\mathrm{meV}] - 28.5\,[\mathrm{meV}]. \tag{38}$$

Lastly, in cyan, we show the range of 90% C.L. upper limits extrapolated from the full KamLAND-Zen [114] dataset. We note here that the upper and lower values of this range come from different theoretical models employed in the analysis - full details are present in Ref. [114].

$$m_{\beta\beta,\,\mathrm{KamLAND-Zen}} < 28.4\,[\mathrm{meV}] - 122\,[\mathrm{meV}]. \tag{39}$$

Appendix: E

$$S_1 = \frac{1}{3}\left(1+\sqrt{4+6(1-3\epsilon)\epsilon}+3\epsilon\right)\tilde{m}_2 + \frac{1}{3}\left(2-\sqrt{4+6(1-3\epsilon)\epsilon}-3\epsilon\right)(m_1\cos^2\theta+\tilde{m}_3\sin^2\theta),$$

$$S_2 = \frac{1}{6}\left(4+\sqrt{4+6(1-3\epsilon)\epsilon}-6\epsilon\right)\tilde{m}_2 + \frac{1}{6}\left(2-\sqrt{4+6(1-3\epsilon)\epsilon}+6\epsilon\right)(m_1\cos^2\theta+\tilde{m}_3\sin^2\theta)$$
$$+\frac{\sqrt{3}}{12}\left(\sqrt{4-6\epsilon}-2\sqrt{1+3\epsilon}\right)(m_1-\tilde{m}_3)e^{i\phi}\sin 2\theta,$$

and

$$S_3 = \frac{1}{6}\left(4+\sqrt{4+6(1-3\epsilon)\epsilon}-6\epsilon\right)\tilde{m}_2 + \frac{1}{6}\left(2-\sqrt{4+6(1-3\epsilon)\epsilon}+6\epsilon\right)(m_1\cos^2\theta+\tilde{m}_3\sin^2\theta)$$
$$-\frac{\sqrt{3}}{12}\left(\sqrt{4-6\epsilon}-2\sqrt{1+3\epsilon}\right)(m_1-\tilde{m}_3)e^{i\phi}\sin 2\theta, \qquad (43)$$

respectively. For $\epsilon = 0$ we recover $S_1 = S_2 = S_3 = \tilde{m}_2$ as expected.

Appendix: F

$$\Delta S_{NO} = 1 - \left[\frac{1}{3m_2}\right]\Bigg(\Big[A^2m_2^2 + B^2m_3^2\sin^4\theta + 2ABm_2m_3\sin^2\theta\cos 2\alpha\Big]^{\frac{1}{2}} + \Big[C^2m_2^2 + D^2m_3^2\sin^4\theta + E^2m_3^2\sin^2 2\theta + 2CDm_2m_3\sin^2\theta\cos 2\alpha - 2CEm_2m_3\sin 2\theta\cos(2\alpha-\phi) - 2DEm_3^2\sin^2\theta\sin 2\theta\cos\phi\Big]^{\frac{1}{2}} + \Big[C^2m_2^2 + D^2m_3^2\sin^4\theta + E^2m_3^2\sin^2 2\theta + 2CDm_2m_3\sin^2\theta\cos 2\alpha + 2CEm_2m_3\sin 2\theta\cos(2\alpha-\phi) + 2DEm_3^2\sin^2\theta\sin 2\theta\cos\phi\Big]^{\frac{1}{2}}\Bigg). \tag{50}$$

Similarly, in the IO case where $M_{diag} = diag.(m_1, m_2e^{2i\alpha}, 0)$, the measure of the degree to which the magic texture symmetry is broken is given by

$$\Delta S_{IO} = 1 - \left[\frac{1}{3m_2}\right]\Bigg(\Big[A^2m_2^2 + B^2m_3^2\cos^4\theta + 2ABm_2m_3\cos^2\theta\cos 2\alpha\Big]^{\frac{1}{2}} + \Big[C^2m_2^2 + D^2m_3^2\cos^4\theta + E^2m_3^2\sin^2 2\theta + 2CDm_2m_3\cos^2\theta\cos 2\alpha + 2CEm_2m_3\sin 2\theta\cos(2\alpha-\phi) + 2DEm_3^2\cos^2\theta\sin 2\theta\cos\phi\Big]^{\frac{1}{2}} + \Big[C^2m_2^2 + D^2m_3^2\cos^4\theta + E^2m_3^2\sin^2 2\theta + 2CDm_2m_3\cos^2\theta\cos 2\alpha - 2CEm_2m_3\sin 2\theta\cos(2\alpha-\phi) - 2DEm_3^2\cos^2\theta\sin 2\theta\cos\phi\Big]^{\frac{1}{2}}\Bigg). \tag{51}$$

Appendix: G

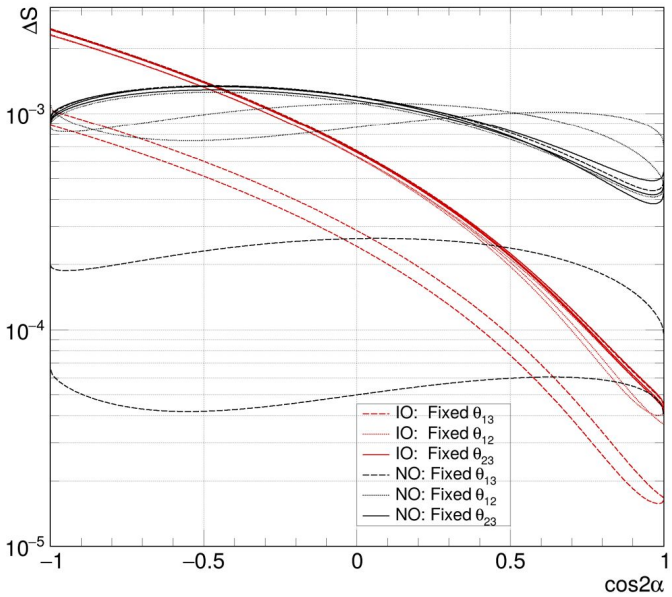

Figure 4: ΔS vs $\cos(2\alpha)$ in the NO(black) and IO(red) scenarios .

Here the curves in the NO and IO case which have the smallest average value correspond to the smallest value of ϵ, as expected. It may also be seen that for small values of α the magic texture symmetry is preserved best. If it is indeed more natural that the violation of this symmetry is minimized, and that in turn α should be small, then the expected value of $m_{\beta\beta}$ in the IO case should be well within the 90% C.L. regions of both KamLAND-Zen and the planned next generation XLZD experiment. On the contrary in the NO case, even for small α, $m_{\beta\beta}$ is expected to fall outside the 90% C.L. region for GERDA, KamLANDm and XLZD, though in the case of XLZD only marginally.

Appendix: H